Article

Predicting the related parameters of vortex bladeless wind turbine by using deep learning method

Mahsa Dehghan Manshadi[1], Majid Ghassemi [1], Seyed Milad Mousavi [1], Amir Mosavi [2*]

1 Department of Mechanical Engineering, K.N.Toosi University of Technology, Tehran, Iran mahsadehghan@email.kntu.ac.ir ; Miladmousavi@email.kntu.ac.ir;
2 John von Neumann Faculty of Informatics, Obuda University, 1034 Budapest, Hungary
* Correspondence: amir.mosavi@uni-obuda.hu;

Abstract: Energy harvesting from wind turbines has been explored by researchers for more than a century from conventional turbines up to the latest bladeless turbines. Amongst these bladeless turbines, vortex bladeless wind turbine (VBT) harvests energy from oscillation of a turbine body. Due to the novelty of this science and the widespread researches around the world, one of the most important issues is to optimize and predict produced power. To enhance the produced output electrical power of VBT, the fluid-solid interactions (FSI) were analyzed to collect a dataset for predicting procedure. Long short-term memory (LSTM) method has been used to predict the produced power of VBT from the collected data. The reason of choosing LSTM from various artificial neural network methods is that the parameters of VBT study are all time- dependent and the LSTM is one of the most accruable algorithms for predicting time series data. In order to find the relationship between the parameter and the variables used in this research, a correlation matrix was presented. According to the value of 0.3 for the root mean square error (RMSE), a comparative analysis between the simulation results and its prediction shows that the LSTM method is very accurate for these types of research. Furthermore, the LSTM method has significantly reduced the computation time so that the prediction time of desired values has been reduced from an average of 2 and a half hours to two minutes. Also, one of the most important achievements of this study is to suggest a mathematical relation of VBT output power which helps to extend it in a different size of VBT with a high range of parameter variations.

Keywords: Computational fluid dynamic; Long short term memory; Vortex bladeless wind turbine; Prediction; Correlation matrix.

1. Introduction

These days, global warming due to the environmental pollution caused by fuels, is one of the crucial issues of development countries [1]. Hence, using renewable energy devices as an energy converter has become common recently. The prevalent renewable energy sources such as wind power, ocean wave power, biomass power and photovoltaic power [2]. One of the most accessible sources of the sustainable energy among introduced sources is wind power. Several projects have been done in a large-scale to utilize these sources all over the world [3]. Although the conventional wind turbines are so costly and have a bad environmental effect [4], researchers have been founding a way to design a type of turbine which is cheap and economical [5]. This important issue inspired engineers to excogitate a vortex bladeless wind turbine (VBT) [6].

VBT is one of the newest bladeless turbines proposed by researchers, which is the beginning of a great revolution in this industry. This type of turbine does not have the problems of the previous generation turbines, so to optimize VBT [7], many researchers around the world have started experimental and research studies. Antony and Boucher [8] have studied the effective parameters on the output power of the bladeless turbine. They showed that for higher and lower wind speeds, the turbine vibration parameters are constant. The results of numerical solution of the equations demonstrate that high amplitudes occur only in vibration resonance. Sassi et al. [9] have utilized discrete element method with immersed boundary method to solve Navier-Stokes equations. By analyzing different vibrational parameters and solving differential equations by Runge-Kutta method, they have concluded that the efficiency values are between 20% and 30% in lock-in range. Gautam et al. [10] performed numerical analyses on the electrical part and the production of turbine power without blades using commercial software. They found that the design of an electromechanical conversion system was essential to achieve the maximum electrical output for a given vibration frequency. They concluded that the different field settings with respect to the coil are crucial for the use of electrical power. Moradi Gharghani et al. [11] have studied the effect of dimensionless Reynolds number on the body oscillation. They concluded that there is a unique Reynolds number for which the frequency of the vortices is equal to the maximum frequency of the turbine oscillation and the maximum power happens . Among these studies, the relationship between the multi-physic parameters, i.e. wind flow velocity in an oscillation amplitude and frequency, wind flow velocity in output power, drag force in an oscillation amplitude and frequency, has not yet been clarified, so it is not evident which one is significant in these kinds of simulations.

Due to the attractiveness of this issue for investors in the field of renewable energy around the world [12] and the significant progress of this type of turbine by experts in this field, it is necessary to conduct more extensive studies on various aspects of this project, to expand these turbines in help around the world. One of the most important areas that can be mentioned for the optimization of VBT is to maximize the production power. Therefore, in order to use the effective parameters on the output power optimization which has not been studied so far, it is necessary to form a new study. Accordingly, this study discussed on how to estimate the power output and mitigate the effective parameters on its efficiency are two essential issues in the VBT improvements.

Investigation of the effects of fluid and solid parameters in the analysis of the fluid-solid interactions (FSI) on the output power of VBT can be done by solving the coupled equations by computational fluid dynamics (CFD) commercial software. In order to predict the optimal amount of generated power, it is necessary to use new methods that have recently been introduced in the field of predicting the amount of electricity generated by energy systems [13], especially wind turbines. In these fields, especially utilizing the output power from wind energy systems several studies were done. Some researchers studied an advanced constructed data-driven model for predicting the output power by using the neural network algorithm [14]. The output power of VBT varies with different parameters i.e. wind flow velocity, rod deflection (oscillation amplitude) and exerted drag force [15]. Therefore, it is crucial to design a suitable algorithm to develop the prediction model. The latest modified method of predicting this type of system is the use of artificial intelligence (AI) [16]. One of the most well-known methods is LSTM [17], and many studies have been performed on this method in optimizing the prediction of output power from wind turbines which is produced by wind turbines in different areas with different geographical properties. Yang et al. [18] have conducted studies on wind power prediction that used the LSTM method for predicting the desired data. They compared the predicted power tables with the available data on the actual turbine power output measured in the wind farm. Wu et al. [19] have studied the effective parameters in optimizing the output power of wind turbines and compared the results with the experimental data available in the wind farm in China. They concluded that the LSTM method can accurately detect values, and that this method is very accurate and fast, and is more efficient at predicting values than other existing methods. Meka et al. [20] have analyzed the information of turbines of a power plant for this research and by drawing diagrams that predict the parameters by LSTM method, they concluded that it is one of the best and most efficient methods in this field. According to the latest studies in this field, it can be concluded that the LSTM method is one of the best methods for VBT analysis, which is one type of wind turbines. The innovation in this research can be justified by the fact that the use of this method in wind turbines without blades has not been mentioned in an article.

To the best of our knowledge, this is the novel study that combined the two-way FSI done by CFD method based on finite element method and its results as a numerical data were used in the LSTM algorithm to have a prediction in produced electrical power by input variables.The novelties of the recent research are;

- The multi-physics numerical analysis in the form of the fluid solid interactions is proposed for the first time by analyzing vortex bladeless wind turbines into the computational fluid dynamic space, which completely demonstrates the fluid parameters of the airflow and can perfectly combine with the most applicable algorithm of deep neural network.
- The long short term memory method is reasonably utilized to predict output electrical power for the first time based on the numerical simulations which can predict the wind power of a vortex bladeless wind turbine. Also, by suggesting a mathematical relation of generated power, much can be done to help the bladeless wind turbine industry to predict output power with less time and cost.

2. Materials and Methods

The VBT is a flexible cylindrical structure which oscillates in a fluid flow [21]. The special type of the VBT 1 meter high was studied in this research [7]. Not only does this special design lack any blades for a rotational movement, but it also has a mast part for oscillating in any direction [22,23]. The vortex shedding phenomenon exerts lift force which causes the structure oscillation to fluctuate crosswise. Using the effect of vortex induced vibration (VIV) phenomenon in an energy harvesting procedure helps to convert fluid energies to the output electrical power by aero-generator. The aero-generator system contains group of moving magnets on a fixed coil which uses Faraday law of an electromagnetic induction [24]. Figure 1 presents the structure of VBT.

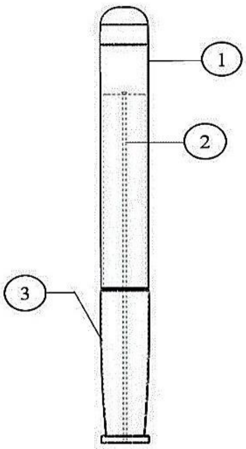

Figure 1. the schematic view of a VBT

As shown in Figure 1, the VBT structure has three main parts that are fixed together:

1. Cylindrical mass made of glass fiber (Part1) [7].
2. flexible rod made of reinforced carbon fiber that is fixed to part1 (Part2) [7].
3. Special cover that anchors the carbon fiber rod to the foundation (Part3) [7].

The purpose of the light weight cylindrical mass that is connected to the flexible rod is to harvest energy by converting the mechanical energy to electrical form of energy.

2.1 Governing Equations

The governing equation is based on assumptions that the air-flow is two-dimensional, steady and incompressible with constant properties considered in 20°C [25]. The two-dimensional continuity equation of fluid is shown as Eq.1 [26].

$$\frac{\partial u}{\partial x}+\frac{\partial v}{\partial y}=0 \tag{1}$$

Where u and v are the wind velocities in x and y directions. In this research, the z-direction velocity (w) was neglected because the VBT doesn't have any vibration in this direction.

The momentum equations in x and y directions are presented as Eq.2 and Eq.3, respectively [26].

$$\frac{\partial u}{\partial t}+u\frac{\partial u}{\partial x}+v\frac{\partial u}{\partial y}=-\frac{1}{\rho}\frac{\partial p}{\partial x}+v\left(\frac{\partial^2 u}{\partial x^2}+\frac{\partial^2 u}{\partial y^2}\right) \tag{2}$$

$$\frac{\partial v}{\partial t}+u\frac{\partial v}{\partial x}+v\frac{\partial v}{\partial y}=-\frac{1}{\rho}\frac{\partial p}{\partial y}+v\left(\frac{\partial^2 v}{\partial x^2}+\frac{\partial^2 v}{\partial y^2}\right) \tag{3}$$

2.2 Computational domain and Boundary conditions

In recent research, the FSI analysis was done by using the transient wind flow as the input. Inlet velocity is considered to have two dimensional variables, and the pressure is assumed constant in the inlet and outlet. Based on these assumptions, the viscosity of the air flow varies with Reynold's number which ,in turn , is a function of different VBT diameters and wind velocity. Related to the input wind velocity, the maximum Reynolds number is 1 · 1 × 105. By considering this maximum value, the flow is assumed to be laminar before having interaction with VBT. When interactions between air flow and VBT happen, the vortex shedding street will change the flow regime to turbulent.

The domain walls are constrained as no-slip boundary condition, but the fluid-structure interfaces are assumed to be slip wall. The study boundary conditions and dimensionless parameters are presented as in Figure 2. The width and the length of the domain are W and H. The upstream distance of the computational domain is designated by W1 while the downstream distance is designated by W2.

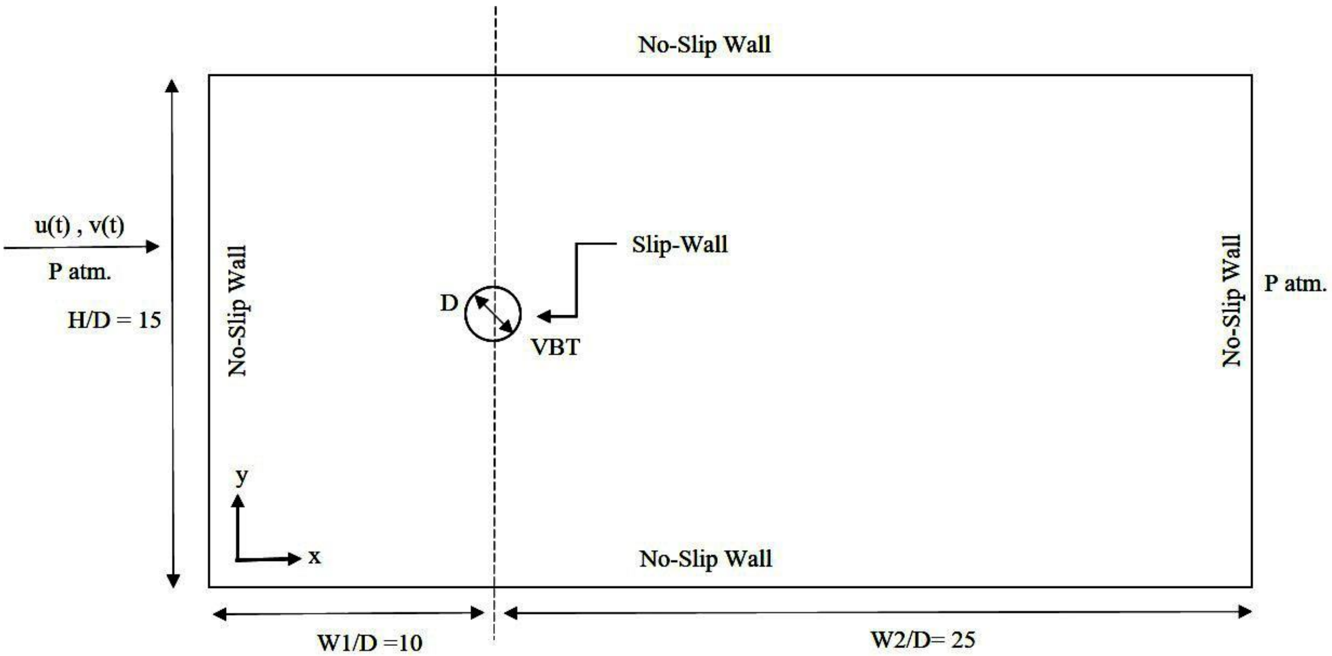

Figure 2. The schematic view of dimensionless parameters and boundary conditions

2.3 Mesh generation and grid independency

Mesh generation analysis essentially acquired the number of a sufficient mesh for purposed study.

Moreover, three different mesh numbers were generated to simulate a VBT which is presented as Table 1.

Table 1. The information about mesh generation

Minimum grid size (m)	Simulation time	Number of elements	Accuracy of oscillation amplitude
0.01	34M 16S	19921	85%
0.005	2H 34M 7S	55848	93%
0.001	5H 54 M 10S	2244300	94%

As presented in Table 1, the number of grids increasesin computational domain in order to increase the accuracy of the numerical simulation. The criterion to select a minimum grid size is to have a high accurate answer due to the least simulation time. Three different triangular type mesh sizes are utilized as given in Table 1. Based on the least simulation time criterion, the 0.05 m grid size with 55848 number of element and about 2 hours and 34 minutes run time is selected [27]. One of the parameters selected to evaluate the accuracy is the oscillation amplitude. Because the accuracy of the selected grid size is as high as the minimum one, the 55848 elements were selected because of the low calculation time and cost.

2.4 Energy conversion between fluid and structure

Energy conversion in wind turbines has the general meaning of converting the wind mechanical energy to output electrical energy. In VBT systems, the wind mechanical energy converts to output electrical energy by using the body vibration. Figure 3 depicts the schematic of the simplified VBT model which is considered as a simple spring-damper model.

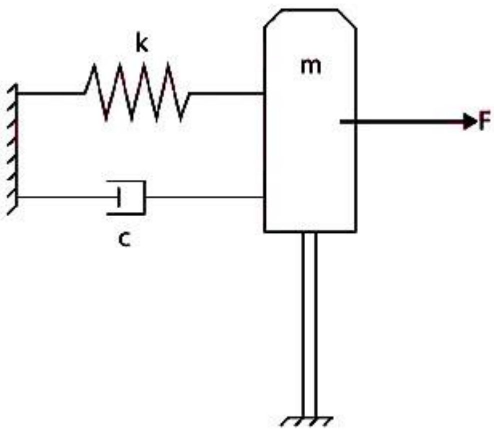

Figure 3. The simplified vibrational system of VBT

Where "m", "k", "c" and F are the mass of the vibrational parts of VBT, the structural stiffness and the wind force which causes the VBT to vibrate, respectively. The general structure vibration equation presented in y-direction is as follow [28]:

$$m\ddot{y} + ky + c\dot{y} = F_{fluid}(x, y, t) \tag{4}$$

The direction of vibration of the VBT is perpendicular to the direction of the wind. The wind flow is presented in x-direction to simplify the equations. Respectively, another direction will be analyzed the same. The force exerted by the fluid is determined as follow [29]:

$$F_{fluid}(x, y, t) = \frac{1}{2}\rho u^2 (Dl) C_d(x, y, t)\hat{\imath} + \frac{1}{2}\rho v^2 (Dl) C_d(x, y, t)\hat{j} \tag{5}$$

Hence, the inlet velocity assumed variable with time and the interfaces of the VBT are same in different direction because of the symmetric shape of the cylinder where ρ is the flow density and is constant, D is the VBT bigger diameter and l is the VBT height. Due to symmetrical shape of the cylinder, it can be proven that the VBT interfaces are same in all direction. Therefore, the vibration is independent of the wind flow direction. $Cd(x.\ y.t)$ is the drag coefficient as is given by a harmonic equation which presents as Eq.6.

$$C_d(x, y, t) = C_d(x, y)\sin(\omega t + \varphi) \tag{6}$$

This equation is considered as a harmonic one , so we have the sine term inside it. φ is the phase angle and ω is angular velocity which is larger than regular frequency f by a factor of 2π.

$$\omega = 2\pi f \tag{7}$$

Where f is the flow frequency. By substituting Eq. 6 in Eq. 5, the Eq. 8 is obtained [28].

$$F_{fluid}(x, y, t) = \frac{1}{2}\rho u^2 (Dl) C_d(x, y)\sin(\omega t + \varphi)\hat{\imath} + \frac{1}{2}\rho v^2 (Dl) C_d(x, y)\sin(\omega t + \varphi)\hat{j} \tag{8}$$

VIV is a phenomenon that occurs with coupling between vortex shedding and structural vibration. Figure 4 presents the schematic of the VBT, the two-way fluid-solid interactions and the vortex shedding effect [29].

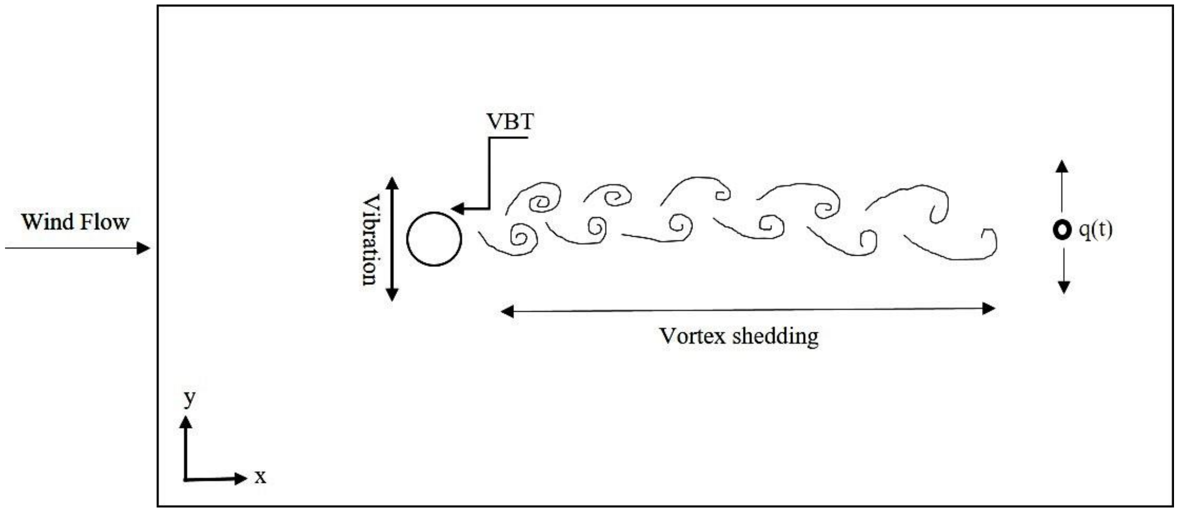

Figure 4. The schematic of two-way effect of vortex induced vibration

The vortex shedding by vibration is a phenomenon that occurs when fluid interact with the vibrational structural and is a function of Reynolds number. The coupled two equations of the VIV phenomenon describing the effect of wind flow on the VBT structures and vice versa are as follows [30]:

$$m\ddot{y} + ky + c\dot{y} = \frac{1}{2}\rho u^2 (Dl) C_d (x, y) \sin(\omega t + \varphi)\hat{\mathrm{i}} + \frac{1}{2}\rho v^2 (Dl) C_d (x, y) \sin(\omega t + \varphi)\hat{j}$$

$$\ddot{q} + \varepsilon\omega_f (q^2 - 1)\dot{q} + \omega_f{}^2 q = A\ddot{y} \tag{9}$$

Where ωf is the vorticity angular velocity and q is the strength of the vortices behind VBT. Eq.12 shows the strength of the vortices.

$$q = 2\frac{c_1}{c_{l_0}} \tag{10}$$

Cl and $Cl0$ are the lift coefficient and constant amplitude.

It should be noticed that the VIV phenomenon depends on some different structural and fluid parameters such as the flow velocity to the structure stiffness. Hence, replacing the experimental value of some parameters can help to simplify the procedure of these coupled equations [31].

The system of non-linear and differential coupled equations of solid and fluid was solved by the 4th order Runge-Kutta method by commercial software.

2.5 Energy harvesting

One of the main parts of this research is numerical analysis of harvesting electrical energy from the VBT vibration while wind flows in a domain. To gain this purpose, the Faraday law of induction is used in order to help determine the electrical energy harvested from the VBT vibration. The mechanical power absorbed by the VBT (Pwind), and the produced electrical power (PVBT) are as follows, respectively [32]:

$$P_{VBT} = \eta P_{wind} \tag{11}$$

$$P_{VBT} = \eta \frac{1}{2}\rho u^3 (2y + D) l \tag{12}$$

2.6 Machine Learning method

One of the essential goals in AI methods is to design an algorithm for building a relationship between input and output data. By utilizing the numerical analysis, the dataset was imported to the AI algorithm to then predict the output parameters.

The selected algorithm for recent study was Long Short-Term Memory (LSTM). LSTM is one of the Deep Neural Network (DNN) methods applicable for detecting different types of time series data [33]. It fundamentally uses a multilayer neural network to learn a time series relationship between the input and output parameters [34]. The data which is accumulated from the sensors in experiments and simulations are time -dependent , so LSTM is the best algorithm for predicting output data [35]. Hence, this algorithm has a feedback connection unlike other neural networks. In other words, LSTM is practical for the applied architecture in long term dependencies.

The data accumulated from the sensors in experiments and simulations are time dependent , so LSTM is the best algorithm for predicting output data. To store the data information which is used in the long-term storage in hidden layers, the "cell-states" were introduced. As presented in Eq. 15 and 16, ft and it introduce the forget and input gates for controlling the input and output of each cell-state [36].

$$f_t = g(W_f.[h_{t-1}.X_t]+b_f) \tag{13}$$

$$i_t = g(W_i.[h_{t-1}.X_t]+b_i) \tag{14}$$

Where the function g introduces a non-linear sigmoid function which is used during activating procedure. f and i indexes show the forget and input parameters, W and b introduce the weight matrix and bias function, $ht-1$ shows the output vector of the last time step and Xt presents the input vector of the current time step.

To gain the input the current state, Eq. 17 presents the relation.

$$C_t' = \tanh(W_c.[h_{t-1}.X_t]+b_c) \tag{15}$$

In this equation, c index shows the current state of each parameters. Eq. 18 obtains the current cellstate, which is considered as using both of forget and input gates [36].

$$C_t = f_t * C_{t-1} + i_t * C_t' \tag{16}$$

By using the output gate of each cell-state as shown in Eq. 19, the output of long short-term memory is presented as Eq. 20.

$$O_t = g(W_o.[h_{t-1}.X_t]+b_o) \tag{17}$$

o index shows the cell-state output parameters.

$$h_t = O_t * \tanh(C_t) \tag{18}$$

Figure 5 shows the cell-state of the LSTM method in predicting the produced power of VBT.

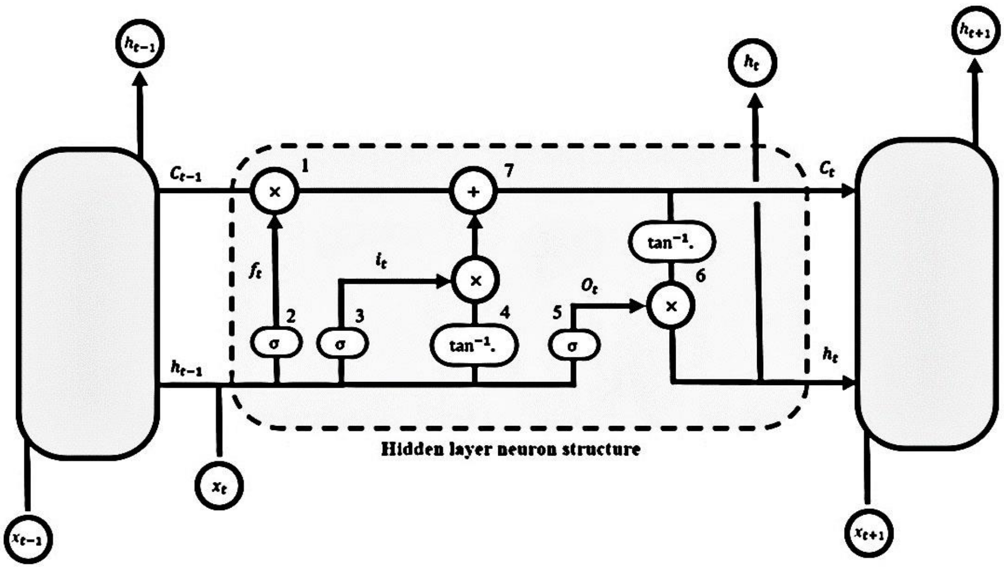

Figure 5. The long short-term memory diagram of a cell-state

In this figure, different operators are indicated as numbers 1-7. Each number demonstrates the different state of data which is shown as Table 2.

Table 2. The definition of different signs on Figure 8

Number	Definition
1	Forget some cell content

2	compute the forget gate
3	compute the input gate
4	compute the new cell content
5	compute the output gate
6	output some cell content to the hidden state
7	write some new cell content

Different training steps based on LSTM neural network are as follows [37]:

1. The t-1 time data feature is input to the input layer, then the output goes to the main cell of time and finally after calculations the output of t-time cell goes into the last cell which is called t+1 time cell.
2. The output data of hidden neuron layer comes from the input, forget and output gates of each cell.
3. The output results are formed by selecting between output LSTM nodes in the last neuron layer.
4. The error is back -propagated during the updating procedure of weight functions.

In this research, 5 hidden layers were selected , containing 10 neurons within the first layer. The epoch size is 200 and walk-forward validation method were used. The back propagation algorithm was utilized for administrated learning technique. Hence, the quantity reduction procedure of the input data was done by Mahalanobis distance (MD) method to reduce the training and prediction time of the whole network [38]. Then, the data collected from numerical analysis would be compared with the predicted data from LSTM method. Finally, the residual signal is applied on a detection step of the occurrence of faults.

3. Results and discussion

In the present research, the numerical solutions were done to collect data for using in the LSTM algorithm. The selected dataset contains the data of 200 seconds of VBT simulation in flow. However, the electrical output power was calculated by utilizing a relation of the generator output power. The datasets have fewer data stores than expected in a case of the real industrial problems.

Due to the comparability of this study, it was preferred that the simulation results and the LSTM predictions are presents in the same figure for each studied parameter. In order to find the relationship between the parameter and the variables used in this research, it was necessary to use a correlation matrix. In this matrix, each row and column represents a parameter and each element of the matrix represents a graph that shows the relationship between them shown as in Figure6. Testing time, wind flow speed (m/s), drag force (N), the VBT vibration amplitude (m) are the parameters analyzed in a correlation matrix and expressed in a value between 0 to 1.

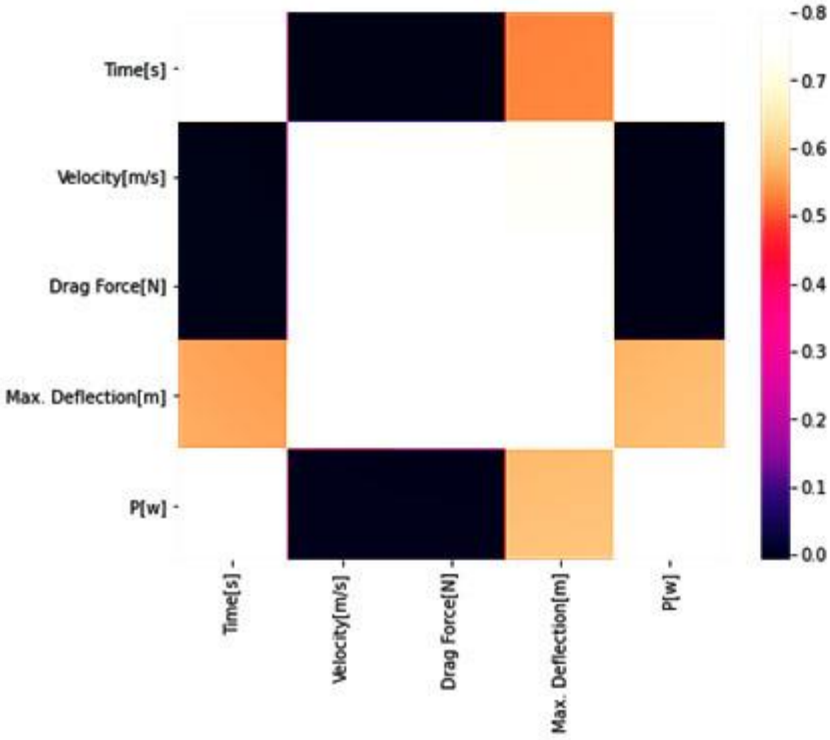

Figure 6. The correlation matrix of different parameters.

As shown in Figure 6, this matrix shows the relation of different quantities with heat-map visualization. It demonstrates the magnitudes with colors from lighter to darker one. The lighter color shows the best relation so it is easy to infer that the prediction procedure finds a good relation between time and output power.

The results of data prediction are presented by graphs. Figure7 shows the scatter plot of predicted magnitudes. It should be noticed that the positive magnitudes of wind flow speed and drag force have been evaluated by numerical solutions but the AI method has predicted both negative and positive values. Also, Fig. 8 shows the linear regression of the correlation scatter data. This figure is the same as Figure 8 but the points are connected with the best fitting line.

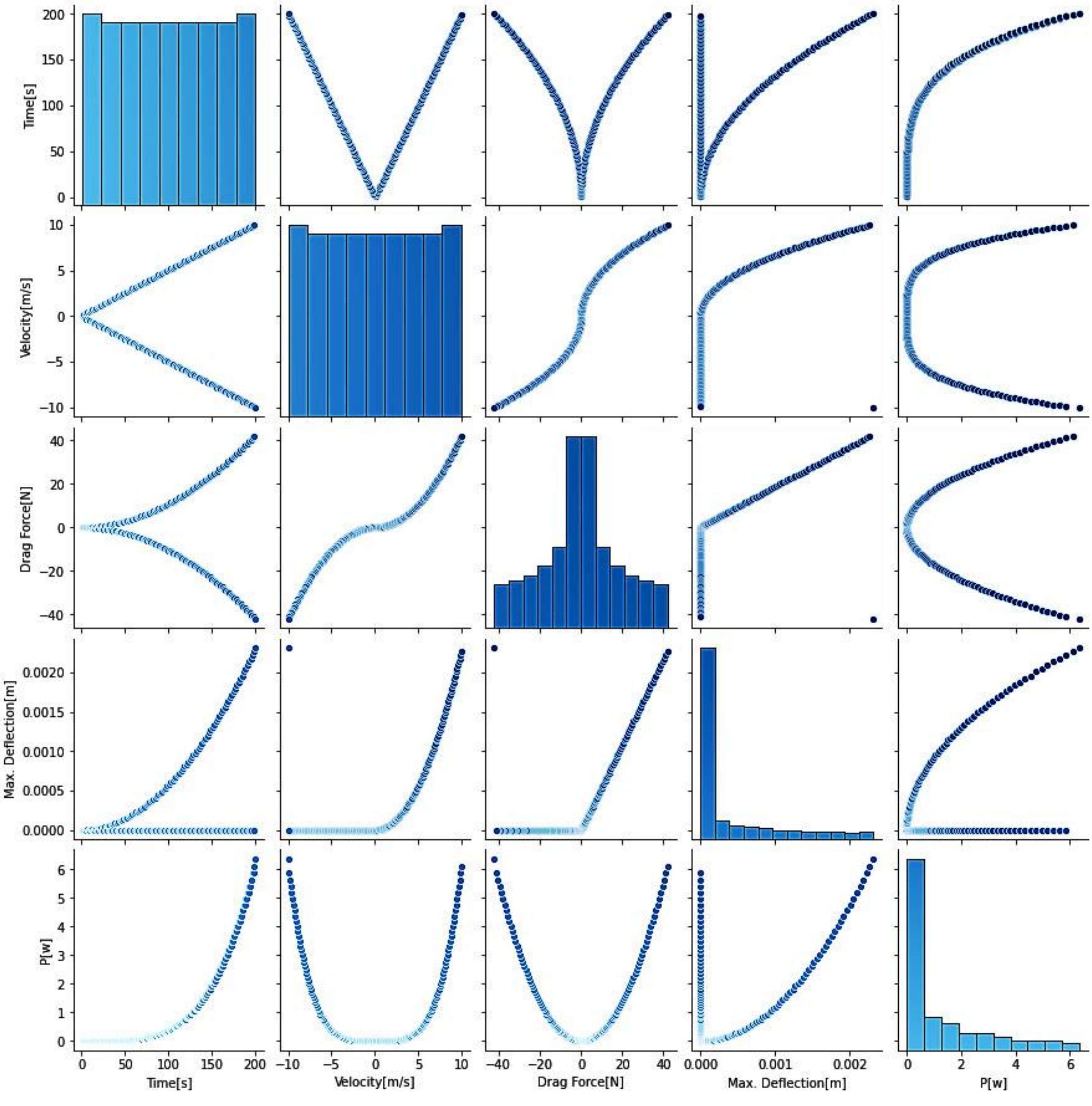

Figure 7. The overall figures of different parameter's correlations.

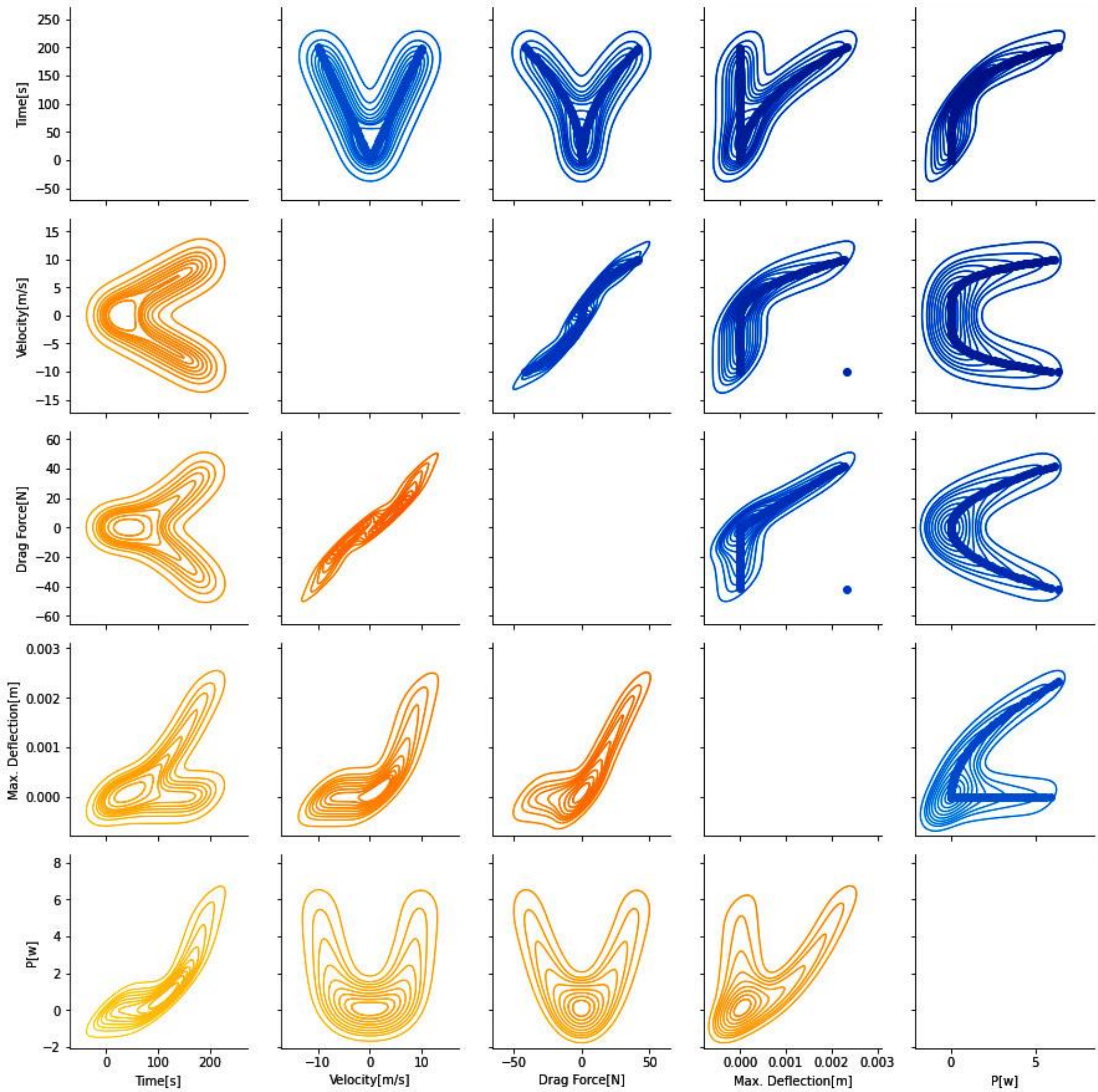

Figure 8. The overall figures of different parameter's correlations.

Figure 8 presents a gradient descent of different variables by optimizing the cost function. These charts show how the answers are optimized to find the best fit ones. To evaluate the effectiveness of the prediction method, the numerical analysis data which is collected from the FSI simulation of VBT has been compared with LSTM method results. The Mahalanobis distance parameter is a combination of produced electrical power, wind flow velocity, amplitude and drag force as an algorithm input dataset. The statistical details of count, mean, and standard deviation of the generated power are shown in Table 3. The mean and median magnitude of generated electrical power are 1.2 and 0.38 w which are related to the information about VBT [33].

Table 3. Statistical descriptions of numerical solution

Name	Power (kw)
Count	200
Mean	1.242593
Standard Deviation	1.669378
Minimum	0.00
25%	0.023927
Median (50%)	0.382359
75%	1.934792
Maximum	6.364972

Figure 9 describes the output electrical power curve from VBT. It presents that the power is the third order function of the input wind flow velocity in the range of 0 to 10 *m/s*. Hence, producing the electrical power in this special type of wind turbine starts from the low value of velocity. It should be noticed that the accuracy of prediction modeling is not only investigated by modeling parameters, but also by the way of input selected variables is an important issue. In other words, another important factor which can impress the produced power is an oscillating amplitude. In this figure, the validation was done and it shows the good agreement. Furthermore, the respective equation is shown on curve.

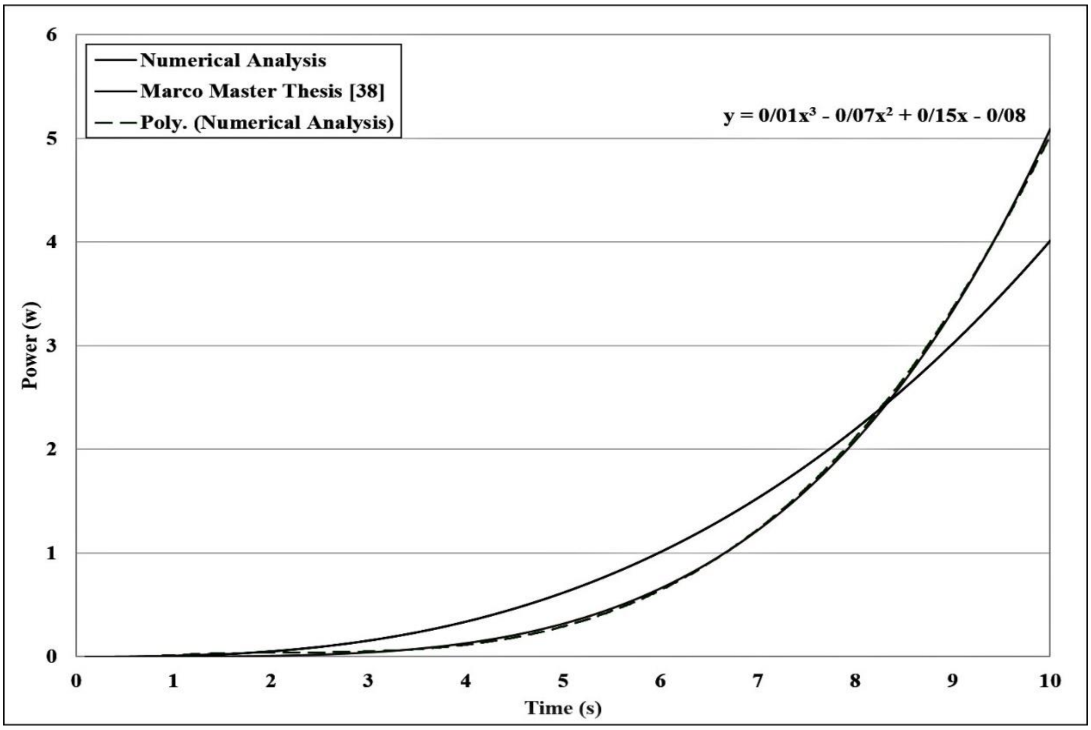

Figure 9. The effect of increasing the wind flow velocity on produced power

Suggesting a mathematical relation between VBT output power and time is one of the novelties of recent research which can be introduced as Equation 21. This equation consists of 180 generated data curve fittings during the LSTM analysis.

$$P = 0/0103t^3 - 0/067t^2 + 0/1522t - 0/0803 \qquad (19)$$

Figure 10 presents the effect of changing the amplitude of vibration on output electrical power. It shows that the generated power has the same magnitude for both negative and positive values of VBT deflection.

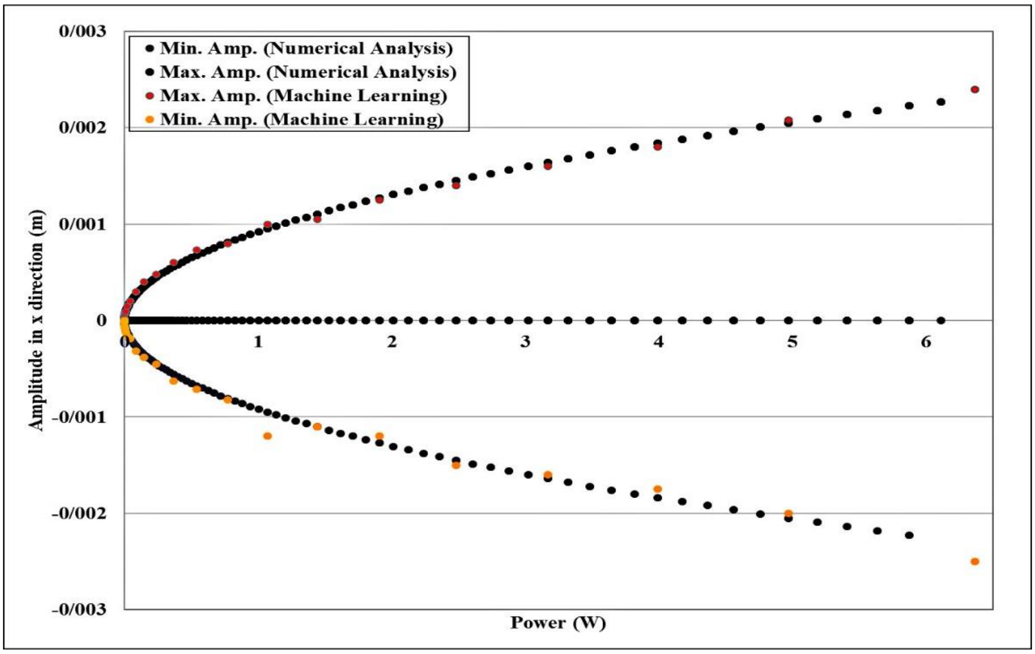

Figure 10. The effect of increasing the produced power on amplitude of vibration

In this case, Figs. 11 to 13 present the effect of the named parameters on each other.

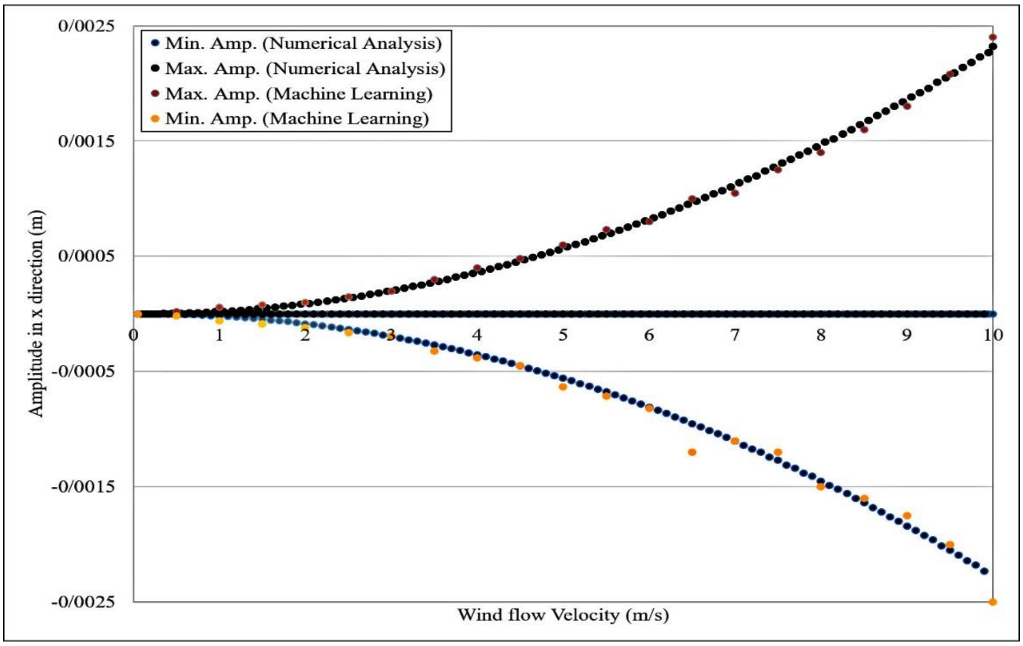

Figure 11. The effect of increasing the wind flow velocity on amplitude of vibration

As shown in Figure 11, the amplitude of the vibration which is caused by the rod deflection increases by increasing the wind flow velocity. The analysis demonstrated all of the parameters change before the lock-in range (10 m/s). As expected by considering the other studies [36], the amplitude of vibration increases to gain 0.0023m at a tip of the VBT. By having comparative analysis of this figure, the predicted values of vibration amplitude are so close to the numerical analysis and it proves that the LSTM method is an accurate one in predicting problems.

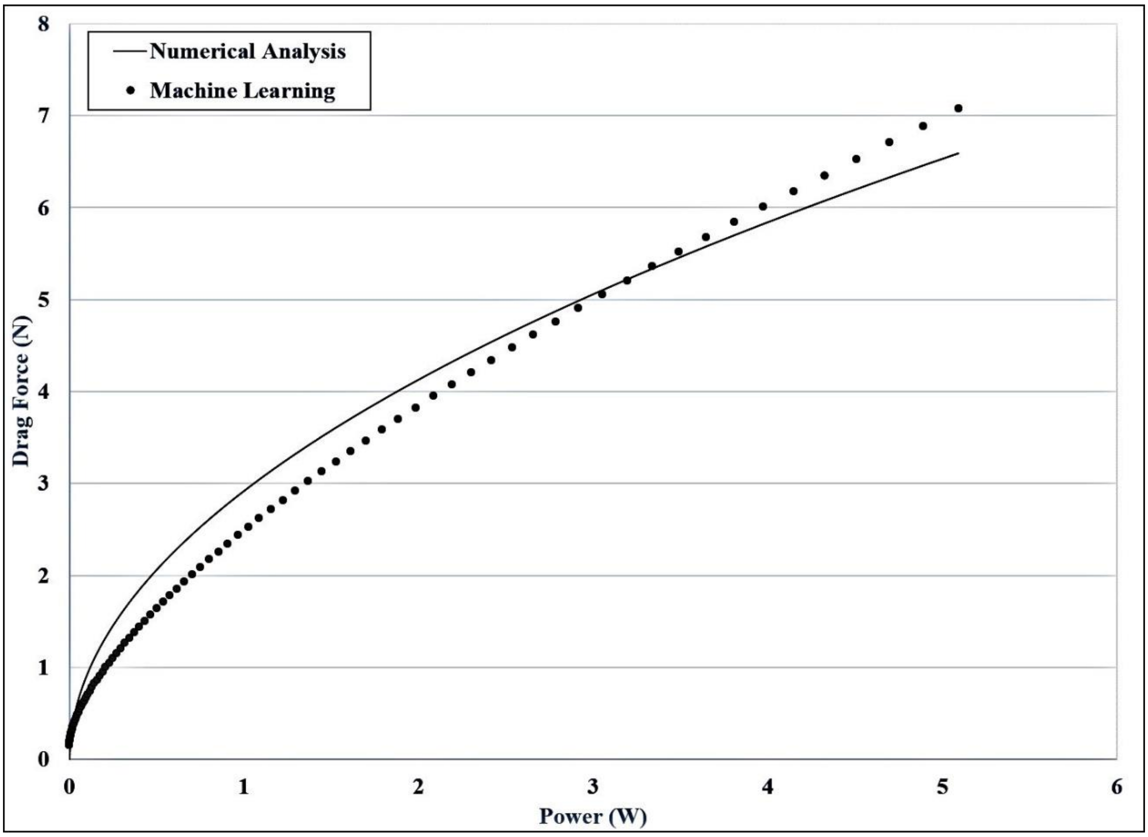

Figure 12. The effect of increasing the produced power on drag force

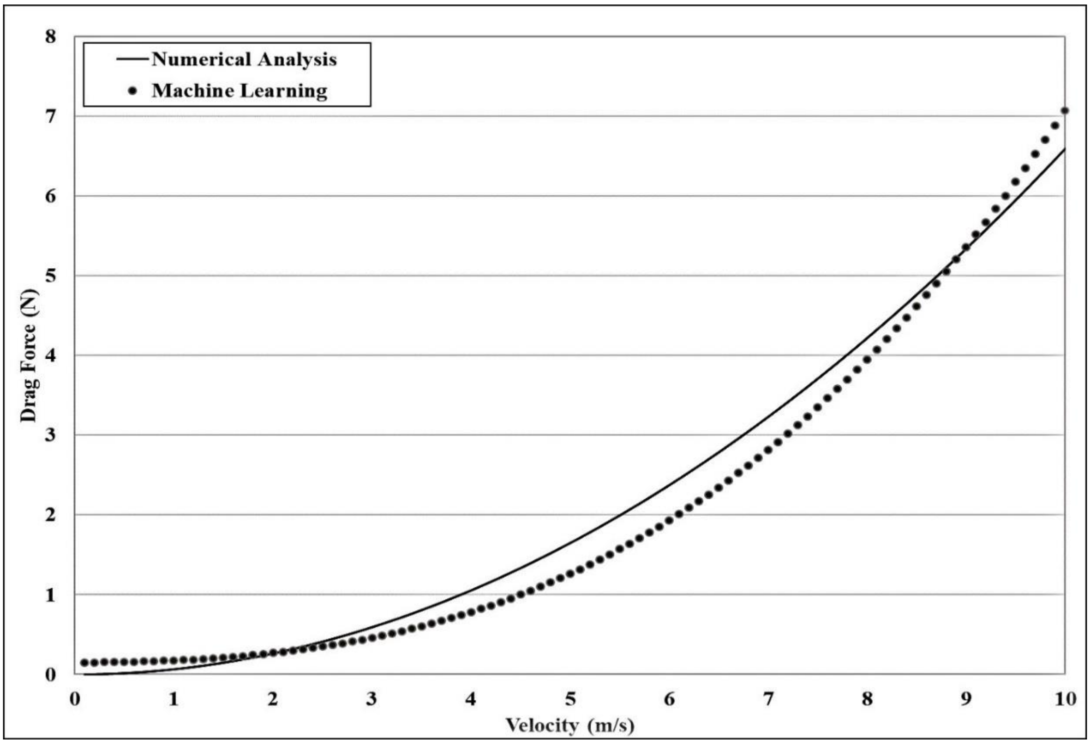

Figure 13. The effect of increasing the wind flow velocity on drag force

As demonstrated in Figure 12, power is the second order function of the drag force. Also, the effect of the wind flow velocity on the exerted drag force was studied in Figure 12. These values obtained from LSTM methods ,presented in discussed figures, were compared with the results of the numerical investigations carried out by CFD-FEM method.

According to the comparative analyses performed for the important parameters in this research, it is possible to understand the performance of the artificial intelligence method by using the concept of root mean square error (RMSE) [22]. Five comparative relationships are explained here as shown in Table 4.

Table 4. The accuracy of LSTM model

Table 4 proves that there is a good agreement between numerical and artificial intelligence method and it can be concluded that the artificial intelligence method is so accurate and fast.

5. Conclusions

Input Variables	RSME Value
Amplitude in x direction, Power Output	0.18
Amplitude in x direction, Wind Speed	0.20
Drag Force, Power Output	0.43
Drag Force, Wind Flow Velocity	0.41
Wind Flow Velocity , Power Output, Drag Force and Amplitude in x direction	0.305

In this paper, a novel machine learning prediction model of the VBT power based on LSTM has been investigated. The dataset has been collected from a numerical analysis which was done by CFD with finite element method in a field of FSI. The best number of grids was chosen for purposed simulation and the calculated generated power was validated with the other study. Hence, different effective parameters which can affect the produced electrical power of VBT have been investigated. The variation of produced electrical power of VBT was studied with changeable parameters through two different solution methods. It has been proved that the vibration amplitude increased with the increasing wind flow velocity up to the wind velocity received to 10 m/s which is a lock-in phenomenon. This particular point is where the maximum power output produced by this type of turbine occurs. For this reason, engineers and researchers in this field are trying to design this type of turbine so that the maximum vibrations of the VBT structure occur in this particular interval. In this study, the lock-in range occurs at a speed of 10 meters per second and the amplitude of the oscillation at this speed is about 0.0025 meters. According to these concepts and studies, the power at this particular point is about 5 watts.

In this study, two different methods were compared and the main goal of this research is to have a comparative analytical solution for simulating the VBT through predicting the power. The prediction procedure has been done by using different effective parameters based on derived LSTM algorithm. The correlation matrix presents the relation of different parameters. By utilizing the RMSE value, it has been shown that they were in a good agreement with the results of the numerical analysis. For comparative analysis between two methods, RSME value of the parameters was calculated and the mean value was obtained to be 0.3. This value proves the very high efficiency of this method in predicting the desired values. The use of this new, fast and cheap method causes the study and industrial work in the field of bladeless wind turbines to be done with much higher accuracy than numerical methods.

This section is not mandatory but may be added if there are patents resulting from the work reported in this manuscript.

Author Contributions: M.D and M.G. proposed the main idea. M.D. and S.M.M. completed the simulation. Methodology, M.D and A.M Software, S.M.M,M.D. Supervision, M.G. The manuscript was written through contributions of all authors.

Declaration of interests: The authors declare that they have no known competing financial interests or personal relationships that could have appeared to influence the work reported in this paper.

Reference

1. Manisalidis I, Stavropoulou E, Stavropoulos A, et al. Environmental and health impacts of air pollution: a review. Frontiers in public health. 2020;8. https://doi.org/10.3389/fpubh.2020.00014
2. Berk I, Kasman A, Kılınç D. Towards a common renewable future: The System-GMM approach to assess the convergence in renewable energy consumption of EU countries. Energy Economics. 2020;87:103922. https://doi.org/10.1016/j.eneco.2018.02.013
3. Martin S, Jung S, Vanli A. Impact of near-future turbine technology on the wind power potential of low wind regions. Applied Energy. 2020;272:115251. https://doi.org/10.1016/j.apenergy.2020.115251
4. Jahangir MH, Shahsavari A, Rad MA. Feasibility study of a zero emission PV/Wind turbine/Wave energy converter hybrid system for stand-alone power supply: A case study. Journal of Cleaner Production. 2020;262:121250. https://doi.org/10.1016/j.jclepro.2020.121250
5. Mostafaeipour A, Rezaei M, Jahangiri M, Qolipour M. Feasibility analysis of a new tree-shaped wind turbine for urban application: A case study. Energy & Environment. 2020 Nov;31(7):1230-56. https://doi.org/10.1177/0958305X19888878
6. Salvador CS, Teresa JA, Martinez JM, et al., editors. Design and Construction of Arc Shaped and Disc Shaped Pendulum for Vortex Bladeless Wind Generator. 2017 25th International Conference on Systems Engineering (ICSEng); 2017: IEEE. https://doi.org/10.1109/ICSEng.2017.39
7. Available from: https://vortexbladeless.com/technology-design/
8. Anthony Adeyanju A., Boucher D. Theoretical Analysis of the Bladeless Wind Turbine Performance. Journal of Scientific Research & Reports. 2020; 26(10): 93-106. https://doi.org/10.9734/JSRR/2020/v26i1030325.
9. Sassi P., Freiría J., Mendina M., et al. Simulation of vorticity wind turbines. Heliyon. 2020;6.
10. Gautam A, Srinivas S and Ravi Teja A. Efficient Electro-Mechanical Conversion System in Bladeless Wind Turbines. 2020 IEEE 29th International Symposium on Industrial Electronics (ISIE). 2020;29:1009-1014. https://doi.org/10.1109/ISIE45063.2020.9152509.
11. Moradi Gharghani F, Bijarchi M and Mohammadi O et al. An experimental investigation into a novelsmall-scale device for energy harvestingusing vortex-induced vibration. International Journal of Low-Carbon Technologies 2020:1–9. https://doi.org/10.1093/ijlct/ctaa060
12. Gibadullin AA, Sadriddinov MI, Kurbonova ZM, Shedko YN, Shamraeva VV. Assessment of factors ensuring sustainable development of the electric power industry in the context of transition to renewable energy sources of the national economy. InIOP Conference Series: Earth and Environmental Science 2020; 421(7): 032051. doi:10.1088/1742-6596/1691/1/012165
13. Mbungu NT, Naidoo RM, Bansal RC, et al. An overview of renewable energy resources and grid integration for commercial building applications. Journal of Energy Storage. 2020;29:101385. https://doi.org/10.1016/j.est.2020.101385
14. Zhou B, Duan H, Wu Q, et al. Short-term prediction of wind power and its ramp events based on semisupervised generative adversarial network. Electrical Power and Energy Systems 2021;125:106411. https://doi.org/10.1016/j.ijepes.2020.106411.
15. Gao Y, Wang M, Ji R, et al. 3-D object retrieval with Hausdorff distance learning. IEEE Transactions on industrial electronics. 2013;61(4):2088-2098. https://doi.org/10.1109/TIE.2013.2262760
16. Hanifi S, Liu X, Lin Z, et al A critical review of wind power forecasting methods—past, present and future. Energies. 2020 Jan;13(15):3764. https://doi.org/10.3390/en13153764
17. Adedeji PA, Akinlabi S, Madushele N, et al. Wind turbine power output very short-term forecast: a comparative study of data clustering techniques in a PSO-ANFIS model. Journal of Cleaner Production. 2020 May 1;254:120135. https://doi.org/10.1016/j.jclepro.2020.120135
18. Mao Yang, Chaoyu Shi, Huiyu Liu, Day-ahead wind power forecasting based on the clustering of equivalent power curves, Energy, 2021:218. https://doi.org/10.1016/j.energy.2020.119515.
19. Wu Q, Guan F, Lv C, Huang Y. Ultra-short-term multi-step wind power forecasting based on CNN-LSTM. IET Renewable Power Generation. 2021 Jan 20. https://doi.org/10.1049/rpg2.12085
20. Meka R, Alaeddini A, Bhaganagar K. A robust deep learning framework for short-term wind power forecast of a full-scale wind farm using atmospheric variables. Energy. 2021 Apr 15;221:119759. https://doi.org/10.1016/j.energy.2021.119759
21. Cajas JC, Houzeaux G, Yáñez D, et al. SHAPE project Vortex Bladeless: Parallel multi-code coupling for fluid-structure interaction in wind energy generation. Adv Comput Eur. 2016:1-6. http://hdl.handle.net/2117/88263
22. Available from: https://vortexbladeless.com/technology-design/
23. Thomai MP, Kharsati L, Rama Samy N, Sivamani S, Venkatesan H. Experimental Analysis of Vortex Induced Vibration in the Bladeless Small Wind Turbine. InASME 2019 Gas Turbine India Conference 2019 Dec 5. American Society of Mechanical Engineers Digital Collection. https://doi.org/10.1115/GTINDIA2019-2484

24. Xu H. Application of intelligent control technology in aero-generator's overload protection. In2020 IEEE International Conference on Information Technology, Big Data and Artificial Intelligence (ICIBA) 2020 Nov 6 (Vol. 1, pp. 309-312). IEEE. https://doi.org/10.1109/ICIBA50161.2020.9276904
25. Available from: https://www.engineeringtoolbox.com/air-properties-d_156.html
26. Singh N. Simulation of flow over a rotationally oscillating square cylinder at low Reynolds numbers. International Journal of Automotive and Mechanical Engineering. 2019;16(1):6368-6385. https://doi.org/10.15282/ijame.16.1.2019.20.0482
27. Hasheminejad SM, Jarrahi M. Numerical simulation of two dimensional vortex-induced vibrations of an elliptic 453 cylinder at low Reynolds numbers. Computers & Fluids. 2015 Jan 31;107:25-42. https://doi.org/10.1016/j.compfluid.2014.10.011
28. Barrero-Gil A, Pindado S, Avila S. Extracting energy from vortex-induced vibrations: a parametric study. Applied mathematical modelling. 2012;36(7):3153-3160. https://doi.org/10.1016/j.apm.2011.09.085
29. Wang J, Geng L, Ding L, et al. The state-of-the-art review on energy harvesting from flow-induced vibrations. Applied Energy. 2020;267:114902. https://doi.org/10.1016/j.apenergy.2020.114902
30. Maftouni N, Dehghan Manshadi M, Mousavi SM. The Effect of Drag Force on The Body Frequencies and The Power Spectrum of a Bladeless Wind Turbine. Transactions of the Canadian Society for Mechanical Engineering. 2021 Apr 13(ja).Tamimi V, Wu J, Naeeni ST, et al. Effects of dissimilar wakes on energy harvesting of Flow Induced Vibration (FIV) based converters with circular oscillator. Applied Energy. 2021;281:116092. https://doi.org/10.1016/j.apenergy.2020.116092
31. Yazdi EA. Nonlinear model predictive control of a vortex-induced vibrations bladeless wind turbine. Smart Materials and Structures. 2018;27(7):075005.
32. Chang Y, Chen J, Qu C, et al. Intelligent fault diagnosis of wind turbines via a deep learning network using parallel convolution layers with multi-scale kernels. Renewable Energy. 2020 Jun 1;153:205-13. https://doi.org/10.1016/j.renene.2020.02.004
33. Kouadri A, Hajji M, Harkat MF, et al. Hidden Markov model based principal component analysis for intelligent fault diagnosis of wind energy converter systems. Renewable Energy. 2020 May 1;150:598-606. https://doi.org/10.1016/j.renene.2020.01.010
34. Chen W, Qiu Y, Feng Y, et al. Diagnosis of wind turbine faults with transfer learning algorithms. Renewable Energy. 2021;163:2053-67. https://doi.org/10.1016/j.renene.2020.10.121
35. Boretto M. Bladeless wind energy conversion (Doctoral dissertation, Politecnico di Torino). 2019.
36. Qian P, Tian X, Kanfoud J, et al. A Novel Condition Monitoring Method of Wind Turbines Based on Long Short-Term Memory Neural Network. Energies. 2019; 12(18):3411. https://doi.org/10.3390/en12183411
37. Mousavi SM, Ghasemi M, Dehghan Manshadi M, Mosavi A. Deep Learning for Wave Energy Converter Modeling Using Long Short-Term Memory. Mathematics. 2021 Jan;9(8):871.